# Direct Torque Control Applied to DFIG Supplied via a Three-Level Inverter Under Random Behavior Wind Speed


**Salah Tamalouzt, Nabil Benyahia, Mariama Said Mohamed, Angel Scipioni, and Bernard Davat**

**Abstract** A doubly fed induction generator (DFIG) driven by a variable speed wind turbine (WT) is presented in this paper. The DFIG is partially interfaced with its rotor via a back-to-back converter. This one is supplied via a three-level inverter in the rotor side and controlled with a flexible algorithm based on DTC technique, to ensure mastery of this generator. The main aim of this contribution is to analyze the performances and robustness of the proposed control technique. The aim of this structure is to obtain at the generator output AC sine waveforms signals with a constant frequency and a low THD, as well as minimum output voltages ripples, regardless of the variation of the wind speed. Indeed, the main objective of this work is the performance analysis of the DTC applied to a three-level inverter in the rotor side of the DFIG considering some constraints that reflect the real operation of the wind turbine generator, such as the randomness behavior of the wind speed, allowing all operation modes of this generator. These operation modes are carried out in a successive and continuous manner, while showing synchronous and overspeed modes. Simulation results, performed under Matlab/Simulink, are presented and analyzed.

## 1 Introduction

The wind power generation systems are among the most effective systems available to generate electricity. Particularly, the DFIG remains widely used in the case of a

S. Tamalouzt (✉)
Laboratoire LTII, Département de Génie Electrique, Faculté de Technologie, Université A/Mira de Bejaia, Bejaia, Algeria

N. Benyahia
Laboratoire LATAGE, Université de M/Mammeri Tizi-Ouzou, Tizi-Ouzou, Algeria

M. Said Mohamed · A. Scipioni · B. Davat
Groupe de Recherche en Electrotechnique et Electronique de Nancy (GREEN), Université de Lorraine, Nancy, France



W. Zamboni, G. Petrone (eds.), *ELECTRIMACS 2019*, Lecture Notes in Electrical Engineering 615, https://doi.org/10.1007/978-3-030-37161-6_7

grid-connected structure. This particularity is due to the potential of delivering high yields in regards to energy production and allowing the independent control of active and reactive power generation [1]. The main advantage of this generator is the size of the power electronic converters that are smaller than those of conventional full-size stator converters. In order to develop an efficient conversion of wind energy connected to the grid, several structures and topologies of converters and control techniques associated with generators of production are proposed in the literature [1–18]. Indeed, the structures based on multilevel inverters improve efficiency and maximize the power delivered to the grid. A multilevel inverter has several advantages over a conventional two-level inverter that uses high switching frequency PWM. Multilevel inverters continue to receive more and more attention because of their high voltage operation capability, low switching losses, high efficiency, and low output of electromagnetic interference. Also, it is possible to verify the good performance of these structures, when supplying the electric grid, by sinusoidal current with less total harmonic distortion (THD), and an adjustable output power factor. Multilevel converters not only can generate the output voltages with very low distortion but also can reduce the $dV/dt$ stress; therefore, electromagnetic compatibility problems can be reduced. They can operate at both fundamental switching frequency and high PWM switching frequency [18–22].

To highlight the advantages of the chosen generator and to develop a wind energy conversion connected to an efficient and economical micro-grid, the control technique selection to adopt is indispensable. One competitive control technique is a direct torque control because of its numerous advantages as a simpler structure with high dynamic performances. Several works have been done in this field [7–15, 18].

Nevertheless, the combination of the WT-DFIG with its converters' advantages and those of DTC applied to a three-level inverter in all operation modes of the DFIG (subsynchronous, supersynchronous, and synchronous mode) in a successive and continuous manner has never been reported in the literature. The evolution of these modes can take long time intervals in a successive and continuous manner, it is why, its study becomes a necessity. Especially, if we want to consider the randomness behavior of the wind speed profile, which is never reported or studied except in [9–12], in which theses modes were studied in a successive and continuous manner, using two-level inverter.

In the field of systems control, the two main handicaps of control techniques can be summed up as follows: The pursuit of references to abrupt changes and the robustness to external and internal disturbances. In this context, the main objectives of this paper are to show the performances and the robustness of the proposed DTC, applied to a WT-DFIG supplied via a three-level inverter, considering the randomness variations of wind speed, allowing the DFIG operation in all modes, while showing synchronous and overspeed modes. That is to show clearly the main advantages of the DFIG with its converter. In addition, the insertion of a three-level inverter to the DFIG will allow the generated signals of very acceptable waveforms and very low THD. Moreover, the quality and performances of this technique are verified to reproduce some constraints that reflect the real operation of the wind,

such as the random variation of the wind speed in the most interesting operating zones of the WT characteristics.

The present work is started with the presentation and description of the proposed system. After that, the models of the WT operation and the DFIG with their control technique are discussed and developed. The effectiveness and the performances of the proposed system are verified by simulation under MATLAB/SIMULINK environment.

## 2 Description of the Proposed System

The proposed overall system is based on a DFIG dedicated to a wind turbine partially interfaced with the grid, via an indirect frequency converter (AC/AC), as illustrated in Fig. 1. This frequency converter consists of two converters separated by an intermediate DC bus, serving as a DC-grid. The first converter (I) is a three-level inverter connected to the rotor of this generator and controlled by the proposed control technique (DTC). Whereas, the connection to the AC-grid is provided via a second converter (II) controlled so as to master its output at an adjustable power factor operation with DC-grid voltage regulation, and to guarantee sinusoidal signals with a constant frequency of 50 Hz.

## 3 Direct Torque Control of the Three-Level Inverter

The objectives of wind turbine controller depend on the operating zone, as described in [1].

The DFIG model expressed in the rotor frame is written as follows in [1, 12].

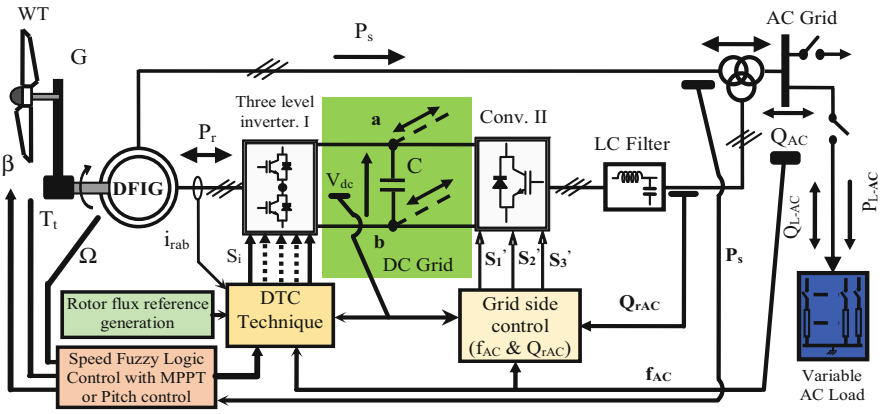


**Fig. 1** Global control scheme

The DTC is based on the rotor flux magnitude regulation and the generator electromagnetic torque value. Where the rotor flux magnitude is estimated from its components along the $\alpha$ and $\beta$ axes, as given in [11]:

$$\begin{cases} \Phi_{r\alpha}(t) = \int_0^t (v_{r\alpha} - R_r i_{r\alpha})\ \mathrm{d}t \\ \Phi_{r\beta}(t) = \int_0^t \left(v_{r\beta} - R_r i_{r\beta}\right)\ \mathrm{d}t \\ \Phi_r = \sqrt{{\Phi_{r\alpha}}^2 + {\Phi_{r\beta}}^2} \end{cases} \tag{1}$$

The electromagnetic torque is given in [1, 11] by the following expression:

$$T_{em} = p\left(\Phi_{r\alpha} i_{r\beta} - \Phi_{r\beta} i_{r\alpha}\right) \tag{2}$$

In order to analyze the output voltage from this three-level inverter, every leg is illustrated by three switches, which permit to independently connect the rotor inputs to the following source voltages ($V_{dc}/2$, 0, and $-V_{dc}/2$).

The transformation into $\alpha\beta$ (or $dq$) subspace obtains a voltage vector that can be associated with the spatial position of the rotor flux. The number of the different states of this vector is 19, because the 8 other combinations produce the same voltage vector. By using the diagonal between the adjacent medium and long vector, it can be seen that the space voltage vector diagram for the three-level inverter is divided into 12 sectors. In Fig. 2, we illustrate an optimal voltage vector, which is selected from the 19 available vectors according to the errors that are set on electromagnetic torque and the rotor flux linkage.

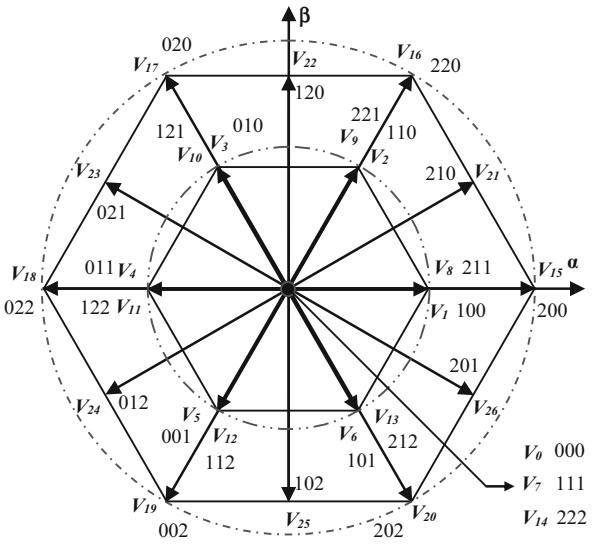


**Fig. 2** Space voltage vectors presentation

The operation of DFIG's direct torque control is characterized by two steps: in one step, the appropriate rotor voltage vector to be applied to the three-stage inverter NPC structure is selected. The other step is characterized by the estimation of the rotor flux and the electromagnetic torque. These estimated values are compared to the respective references, and the errors are used through hysteresis controllers.

The direct torque control of the DFIG topology is based on the hysteresis controller output relating to the variable flux ($C_{\text{flx}}$) and the variable torque ($C_{\text{trq}}$) associated to the sector $N$ corresponding to the rotor flux vector position.

In this paper, we consider that the rotor flux control is achieved by using a three-level hysteresis comparator, while the electromagnetic torque is controlled by using 5-level hysteresis. The inverter state is considered as high if the output of the torque comparator is high or equal to two. Otherwise, the state is low, as given in equations (3) and (4).

$$\begin{cases} \text{If } \Delta tr > \varepsilon_{\text{tr}_2} & \text{Then; } C_{\text{trq}} = +2 \\ \text{If } -\varepsilon_{\text{tr}_1} \le \Delta tr \le \varepsilon_{\text{tr}_2} \ \& \ \frac{\Delta tr}{\text{d}t} > 0 & \text{Then; } C_{\text{trq}} = +1 \\ \text{If } -\varepsilon_{\text{tr}_1} \le \Delta tr \le \varepsilon_{\text{tr}_2} \ \& \ \frac{\Delta tr}{\text{d}t} < 0 & \text{Then; } C_{\text{trq}} = +2 \\ \text{If } 0 < \Delta tr \le \varepsilon_{\text{tr}_1} \ \& \ \frac{\Delta tr}{\text{d}t} > 0 & \text{Then; } C_{\text{trq}} = 0 \\ \text{If } 0 < \Delta tr \le \varepsilon_{\text{tr}_1} \ \& \ \frac{\Delta tr}{\text{d}t} < 0 & \text{Then; } C_{\text{trq}} = +1 \\ \text{If } -\varepsilon_{\text{tr}_1} \le \Delta tr \le 0 \ \& \ \frac{\Delta tr}{\text{d}t} > 0 & \text{Then; } C_{\text{trq}} = -1 \\ \text{If } -\varepsilon_{\text{tr}_1} \le \Delta tr \le 0 \ \& \ \frac{\Delta tr}{\text{d}t} > 0 & \text{Then; } C_{\text{trq}} = 0 \\ \text{If } -\varepsilon_{\text{tr}_2} \le \Delta tr \le -\varepsilon_{\text{tr}_1} \& \ \frac{\Delta tr}{\text{d}t} > 0 & \text{Then; } C_{\text{trq}} = -2 \\ \text{If } -\varepsilon_{\text{tr}_2} \le \Delta tr \le -\varepsilon_{\text{tr}_1} \& \ \frac{\Delta tr}{\text{d}t} > 0 & \text{Then; } C_{\text{trq}} = -1 \\ \text{If } \Delta tr < -\varepsilon_{\text{tr}_2} & \text{Then; } C_{\text{trq}} = -2 \end{cases} \tag{3}$$

$$\begin{cases} \text{If } \Delta\varphi_{\text{r}} > \varepsilon_{\text{flx}} & \text{Then; } C_{\text{flx}} = +1 \\ \text{If } 0 \le \Delta\varphi_{\text{r}} \le \varepsilon_{\text{flx}} \ \& \ \frac{\Delta\varphi_{\text{r}}}{\text{d}t} > 0 & \text{Then; } C_{\text{flx}} = 0 \\ \text{If } 0 \le \Delta\varphi_{\text{r}} \le \varepsilon_{\text{flx}} \ \& \ \frac{\Delta\varphi_{\text{r}}}{\text{d}t} < 0 & \text{Then; } C_{\text{flx}} = +1 \\ \text{If } -\varepsilon_{\text{flx}} < \Delta\varphi_{\text{r}} < 0 \ \& \ \frac{\Delta\varphi_{\text{r}}}{\text{d}t} > 0 & \text{Then; } C_{\text{flx}} = -1 \\ \text{If } -\varepsilon_{\text{flx}} < \Delta\varphi_{\text{r}} < 0 \ \& \ \frac{\Delta\varphi_{\text{r}}}{\text{d}t} < 0 & \text{Then; } C_{\text{flx}} = 0 \\ \text{If } \Delta\varphi_{\text{r}} < -\varepsilon_{\text{flx}} & \text{Then; } C_{\text{flx}} = -1 \end{cases} \tag{4}$$

The electromagnetic torque control is ensured by using a five-level hysteresis comparator, which allows having both directions of machine rotation, the corrector output variable is a Boolean type $C_{\text{trq}}$, it indicates if the electromagnetic torque amplitude must be increased, decreased or maintained constant ($C_{\text{trq}} = 1, 2, 0, -2, -1$), as modeled by Eq. (3). A three-level hysteresis comparator is used to control the rotor flux. The comparator output variable is a Boolean type $C_{\text{flx}}$, it indicates if the rotor flux amplitude must be increased ($C_{\text{flx}} = 1$), decreased ($C_{\text{flx}} = -1$), or

**Table 1** DTC Commutation table of the three-level inverter

| | | $N$ | | | | | | | | | | | |
|---|---|---|---|---|---|---|---|---|---|---|---|---|---|
| $C_{flx}$ | $C_{trq}$ | 1 | 2 | 3 | 4 | 5 | 6 | 7 | 8 | 9 | 10 | 11 | 12 |
| +1 | +2 | $V_{21}$ | $V_{16}$ | $V_{22}$ | $V_{17}$ | $V_{23}$ | $V_{18}$ | $V_{24}$ | $V_{19}$ | $V_{25}$ | $V_{20}$ | $V_{26}$ | $V_{15}$ |
| | +1 | $V_{21}$ | $V_2$ | $V_{22}$ | $V_3$ | $V_{23}$ | $V_4$ | $V_{24}$ | $V_5$ | $V_{25}$ | $V_6$ | $V_{26}$ | $V_1$ |
| | 0 | Zero vector | | | | | | | | | | | |
| | −1 | $V_{26}$ | $V_1$ | $V_{21}$ | $V_2$ | $V_{22}$ | $V_3$ | $V_{23}$ | $V_4$ | $V_{24}$ | $V_5$ | $V_{25}$ | $V_6$ |
| | −2 | $V_{26}$ | $V_{15}$ | $V_{21}$ | $V_{16}$ | $V_{22}$ | $V_{17}$ | $V_{23}$ | $V_{18}$ | $V_{24}$ | $V_{19}$ | $V_{25}$ | $V_{20}$ |
| −1 | +2 | $V_{17}$ | $V_{23}$ | $V_{18}$ | $V_{24}$ | $V_{19}$ | $V_{25}$ | $V_{20}$ | $V_{26}$ | $V_{15}$ | $V_{21}$ | $V_{16}$ | $V_{22}$ |
| | +1 | $V_3$ | $V_{23}$ | $V_4$ | $V_{24}$ | $V_5$ | $V_{25}$ | $V_6$ | $V_{26}$ | $V_1$ | $V_{21}$ | $V_2$ | $V_{22}$ |
| | 0 | Zero vector | | | | | | | | | | | |
| | −1 | $V_5$ | $V_{25}$ | $V_6$ | $V_{26}$ | $V_1$ | $V_{21}$ | $V_2$ | $V_{22}$ | $V_3$ | $V_{23}$ | $V_4$ | $V_{24}$ |
| | −2 | $V_{19}$ | $V_{25}$ | $V_{20}$ | $V_{26}$ | $V_{15}$ | $V_{21}$ | $V_{16}$ | $V_{22}$ | $V_{17}$ | $V_{23}$ | $V_{18}$ | $V_{24}$ |
| 0 | +2 | $V_{22}$ | $V_{17}$ | $V_{23}$ | $V_{18}$ | $V_{24}$ | $V_{19}$ | $V_{25}$ | $V_{20}$ | $V_{26}$ | $V_{15}$ | $V_{21}$ | $V_{16}$ |
| | +1 | $V_{22}$ | $V_3$ | $V_{23}$ | $V_4$ | $V_{24}$ | $V_5$ | $V_{25}$ | $V_6$ | $V_{26}$ | $V_1$ | $V_{21}$ | $V_2$ |
| | 0 | Zero vector | | | | | | | | | | | |
| | −1 | $V_{25}$ | $V_6$ | $V_{26}$ | $V_1$ | $V_{21}$ | $V_2$ | $V_{22}$ | $V_3$ | $V_{23}$ | $V_4$ | $V_{24}$ | $V_5$ |
| | −2 | $V_{25}$ | $V_{20}$ | $V_{26}$ | $V_{15}$ | $V_{21}$ | $V_{16}$ | $V_{22}$ | $V_{17}$ | $V_{23}$ | $V_{18}$ | $V_{24}$ | $V_{19}$ |

maintained constant ($C_{flx} = 0$) so as to maintain: $|\Phi_{r\_ref} - \Phi_r| \leq \Delta\varphi_r$, as given by Eq. (4).

Table 1 represents the commutation table, which is considered as one of the solutions adapted to choose the optimally selected voltage vector for each sector. Where, the rotor flux and the electromagnetic torque are achieved by using, respectively, three levels and five levels hysteresis comparator.

In analyzing the effect of each available voltage vector, it can be seen that the vector affects the electromagnetic torque and the rotor flux linkage with the variation of the module and direction of the selected vector. The nulls voltages vectors ($V_0$, $V_7$, and $V_{14}$) are chosen alternately, so as to minimize the number of commutations in the arms of the inverter [20].

## 4 Simulation Results and Discussion

The effectiveness of the proposed control strategy that leads to better performances of the WT-DFIG system is carried out. Simulations have been realized under wind speed variations, in the aim to allow all the DFIG operation modes in a successive and continuous manner. The WT-DFIG simulation parameters are given in [1]. The DTC strategy presented in the previous paragraph is then introduced, to control the three-level inverter, under MATLAB/SIMULINK environment. The weather data in terms of wind speed profiles are shown in Fig. 3a.

The DFIG mechanical speed is presented in Fig. 3a. The tracking of the references is shown by the mechanical speed, electromagnetic torque, and the rotor

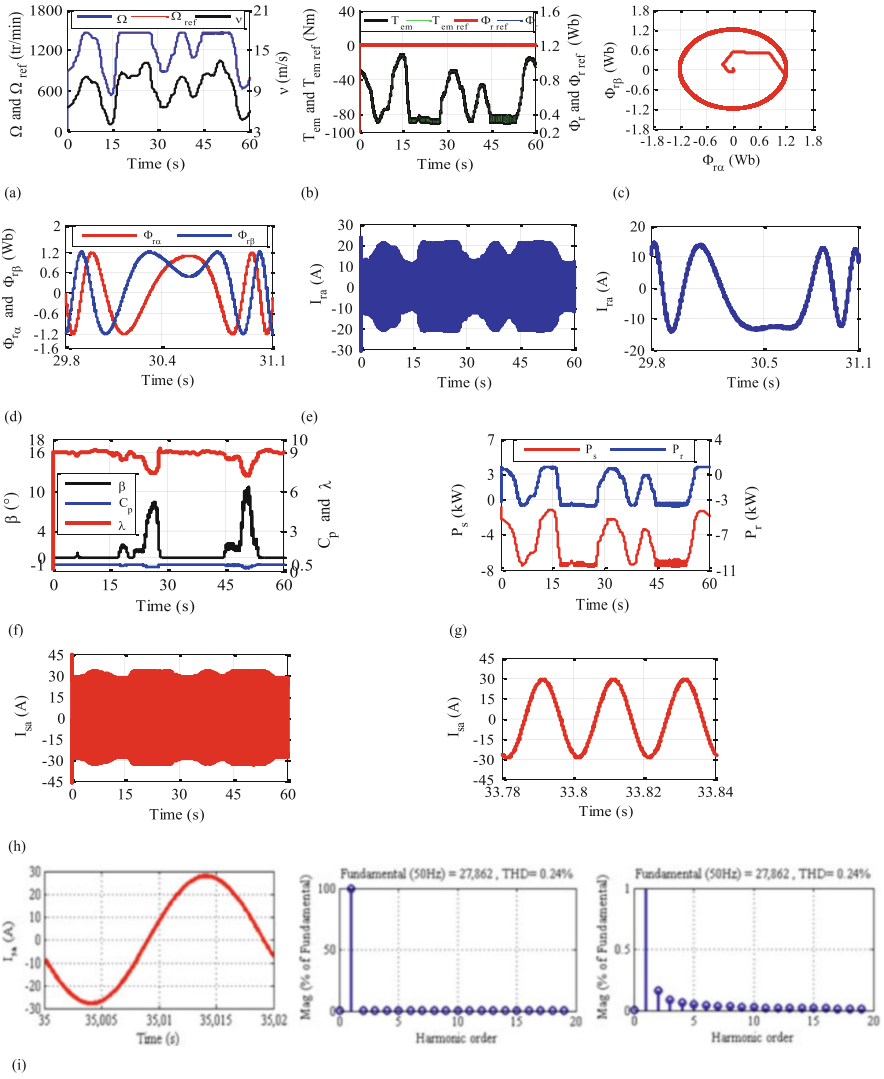


**Fig. 3** Waveforms of the simulation results for a variable wind speed: (**a**) Ω, $\Omega_{\text{ref}}$ and $\nu$; (**b**) $\Phi_{\text{r}}$, $\Phi_{\text{r ref}}$, $T_{\text{em}}$ and $T_{\text{em ref}}$; (**c**) $\Phi_{\text{r}\beta} = f(\Phi_{\text{r}\alpha})$; (**d**) $\beta$, $\lambda$ and $C_{\text{p}}$; (**e**) $P_{\text{r}}$ and $P_{\text{s}}$; (**f**) Zooms of the $\Phi_{\text{r}\alpha}$, $\Phi_{\text{r}\beta}$ in the three modes DFIG operation; (**g**) $I_{\text{ra}}$ and its zoom in the three modes DFIG operation; (**h**) $I_{\text{sa}}$ and its zoom; (**i**) Generated phase current (stator current, $I_{\text{sa}}$) and its harmonic spectrum in supersynchronous mode operation of DFIG

flux magnitude waveforms, as shown, respectively, in Fig. 3a–c. Hence, these results confirm better performances and robustness of the proposed control. Moreover, the torque ripples are about 60% less than the results given in [1, 11].

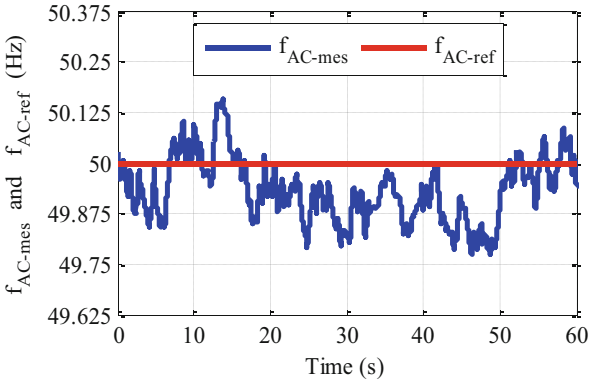


**Fig. 4** The output frequency $f_{AC}$ and its reference $f_{AC\text{-}ref}$

Figure 3c shows the rotor flux waveform, which is circular and kept constant at 1.2 Wb. This form leads to a sinusoidal fluxes $\Phi_{r\alpha}$ and $\Phi_{r\beta}$ behavior (Fig. 3d) in both the sub- and supersynchronous modes. However, in the synchronous mode the rotor fluxes have continuous behavior. Also, this operation mode is proved by a direct form of the rotor phase currents, as presented in Fig. 3e. In these figures, we illustrate the sinusoidal evolution of the rotor currents, in the sub- and supersynchronous operation modes. Besides, the current waveform in Fig. 3e shows good signal quality.

Figure 3f illustrates the $\beta$, $\lambda$, and $C_p$ (blade pitch angle, tip speed ratio, and power coefficient respectively), where one can see that when the power reached its maximum value, the pitch angle control is activated, as presented in Fig. 3g, which shows all the exchanged powers between the grid and DFIG. The $P_s$ depends on the wind speed evolution, whereas, $P_r$ changes its direction, marked by its sign, according the generator slip.

Finally, the sinusoidal form of the generated current shown in Figs. 3h, i and 4 show the quality of the power injected in the AC-grid from the DFIG stator. This remains true also for the three operating modes with a constant 50 Hz frequency. Moreover, the variable amplitude is a consequence of the wind speed variation.

Compared with the results obtained in [1, 11], the proposed DTC associated to the three-level inverter, offers a significant improvement to the stator currents supplied to the AC-grid, with a total harmonic distortion (THD) largely below the limits imposed by IEEE std 519, as illustrated in Fig. 4. This confirms a better quality of energy generated in the AC-grid.

## 5 Conclusions

The performances of the DTC applied to a three-level inverter have been presented in this paper; taking into account the mains advantages of the DFIG when associated with its converter. In this work, the wind speed random variation is imposed in order

to check the quality and performances of this control. Thus, the randomness behavior of the wind speed allowed the utilization of the DFIG in its different operation modes. The study in this paper is focused on the DTC dynamic performances. The effectiveness and validity of this control are verified by numerical simulation using Matlab/Simulink.

The obtained simulation results show that the application of the DTC significantly improves the performance of the conversion system, which contributes to reducing the harmonic distortion rate in the output voltage and current waves and the torque ripples (the generated power).

The results obtained confirm an acceptable robustness of the proposed control, and the performances are satisfactory. The three-level inverter inserted in the DFIG rotor also contributes to improving the quality of the energy supplied to the AC-grid.

## References

1. S. Tamalouzt, N. Benyahia, T. Rekioua, D. Rekioua, R. Abdessemed, Performances analysis of WT-DFIG with PV and fuel cell hybrid power sources system associated with hydrogen storage hybrid energy system. Int. J. Hydrog. Energy **41**(45), 21006–21021 (2016)
2. K.C. Wong, S.L. Ho, K.W.E. Cheng, Direct torque control of a doubly-fed induction generator with space vector modulation. Elec. Power Comp. Syst. **36**(12), 1337–1350 (2008)
3. M. Rahimi, M. Parniani, Dynamic behavior analysis of doubly-fed induction generator wind turbines, the influence of rotor and speed controller parameters. Int. J. Elec. Power Energy Syst. **32**(5), 464–477 (2010)
4. K. Kerrouche, A. Mezouar, K. Belgacem, Decoupled control of doubly fed induction generator by vector control for wind energy conversion system. Energy Procedia **42**, 239–248 (2013)
5. M. Adjoudj, M. Abid, A. Aissaoui, Y. Ramdani, H. Bounoua, Sliding mode control of a doubly fed induction generator for wind turbines. Rev. Roum. Sci. Techn. Electrotechn. et Energ. **56**(1), 15–24 (2011)
6. A. Abdelfetteh, M. Abid, Hybrid fuzzy sliding mode control of a doubly fed induction generator in wind turbines. Rev. Roum. Sci. Techn. Electrotechn. et Energ. **57**(4), 15–24 (2012)
7. J. Arbi, M.J. Ben Ghorbal, I. Slama-Belkhodja, L. Charaabi, Direct virtual torque control for doubly fed induction generator grid connection. IEEE Trans. Ind. Electron. **56**(10), 4163–4173 (2009)
8. J. Ben Alaya, A. Khedher, M.F. Mimouni, Speed-sensorless DFIG wind drive based on DTC using sliding mode rotor flux observer. Int. J. Renew. Energy Res. **2**(4), 735–745 (2012)
9. A.F. Payam, M.N. Hashemnia, J. Faiz, Robust DTC control of doubly fed induction machines based on input-output feedback linearization using recurrent neural networks. J. Power Electron. **11**(5), 719–725 (2011)
10. S. Tamalouzt, T. Rekioua, R. Abdessamed, K. Idjdarene, Direct torque control of grid connected doubly fed induction generator for the wind energy conversion, in *International Renewable Energy Congress IREC'2012*, Sousse, Tunisia, 19–22 Dec. 2012, pp. 1–6
11. S. Tamalouzt, K. Idjdarene, T. Rekioua, R. Abdessamed, Direct torque control of wind turbine driven doubly fed induction generator. Rev. Roum. Sci. Techn. Electrotechn. et Energ. **61**(3), 244–249 (2016)

12. S. Tamalouzt, T. Rekioua, R. Abdessemed, Direct torque and reactive power control of grid connected doubly fed induction generator for the wind energy conversion, in *International Conference on Electrical Sciences and Technologies in Maghreb (CISTEM)*, Tunis, 3–6 Nov. 2014, pp. 1–7
13. J. Hu, X. Yuan, VSC-based direct torque and reactive power control of doubly fed induction generator. Renew. Energy **40**, 13–23 (2012)
14. M. Sandhu, T. Thakur, Multilevel inverters: literature survey – topologies, control techniques & applications of renewable energy sources - grid integration. J. Eng. Res. Appl. **04**(03 (Version 1)), 644–652 (2014)
15. Y. Djeriri, A. Meroufel, B. Belabbes, A. Massoum, Three-level NPC voltage source converter based direct power control of the doubly fed induction generator at low constant switching frequency. Rev. Energ. Renouv. **16**(01), 91–103 (2013)
16. A. Djoudi, S. Bacha, H. Iman-Eini, T. Rekioua, Sliding mode control of DFIG powers in the case of unknown flux and rotor currents with reduced switching frequency. Electr. Power Energy Syst. **96**, 347–356 (2018)
17. L. Gidwani, H. Tiwari, R.C. Bansal, Improving power quality of wind energy conversion system with unconventional power electronic interface. Electr. Power Energy Syst. **44**, 445–453 (2013)
18. N. Taïb, B. Metidji, T. Rekioua, Performance and efficiency control enhancement of wind power generation system based on DFIG using three-level sparse matrix converter. Int. J. Electr. Power Energy Syst. **53**, 287–296 (2013)
19. T. Ghennam, E.M. Berkouk, B. Francois, DC-link voltage balancing algorithm using a space-vector hysteresis current control for three-level VSI applied for wind conversion system, in *2007 European Conference on Power Electronics and Applications*, Aalborg, 2007, pp. 1–10
20. A. Nami, J. Liang, F. Dijkhuizen, G.D. Demetriades, Modular multilevel converters for HVDC applications: review on converter cells and functionalities. IEEE Trans. Power Electron. **30**(1), 18–36 (2015)
21. A. Nami, F. Zare, *Multilevel Converters in Renewable Energy Systems* (In-Tech, Cooperstown, NY, 2010)
22. A. Lega, Multilevel converters: dual two-level inverter scheme, Ph.D thesis in Electrical Engineering, University of Bologna, pp. 39–51, 2007